

MOL #41780

Small Molecule Disruption of G Protein $\beta\gamma$ Subunit Signaling Inhibits Neutrophil

Chemotaxis and Inflammation.

Lehmann, D.M., A.M.P.B. Seneviratne, and A.V. Smrcka* .

Departments of Pharmacology and Physiology (DML and AVS), and Pathology
(AMPBS), University of Rochester, Rochester, New York 14642

MOL #41780

a) Running title: **Targeting PI3-kinase γ Interactions with G β γ**

b) A.V. Smrcka

University of Rochester, Department of Pharmacology and Physiology

601 Elmwood Ave., Box 711

Rochester, NY 14642

Tel.: (585)275-0892

FAX: (585)273-2652

E-mail: alan_smrcka@urmc.rochester.edu

c) Number of text pages: 27

Number of tables: 1

Number of figures: 5

Words in Abstract: 116

Words in introduction: 395

Words in discussion: 721

References: 37

d) Abbreviations: GPCR, G protein coupled receptor; PLC, phospholipase C; bG β γ , N terminally biotinylated G β γ ; PAK1, p21/Cdc42/Rac1-activated kinase 1; PI3-kinase, phosphoinositide 3-kinase; PIP₃, phosphatidylinositol 3,4,5-trisphosphate; GFP-PH-Akt, Green fluorescent protein fusion with the pleckstrin homology domain from Akt protein kinase; NSAID, nonsteroidal anti-inflammatory drug; NCI, National Cancer Institute; IP, inositol phosphate; Cg, carrageenan; IM, indomethacin.

MOL #41780

Abstract

G protein $\beta\gamma$ subunit-dependent signaling is important for chemoattractant-dependent leukocyte chemotaxis. Selective small molecule targeting of PI3-kinase γ catalytic activity is a target of interest for anti-inflammatory pharmaceutical development. Here we examined if small molecule inhibition of $G\beta\gamma$ -dependent signaling, including $G\beta\gamma$ -dependent activation of PI3-kinase γ and Rac1, could inhibit chemoattractant-dependent neutrophil migration *in vitro* and inflammation *in vivo*. Small molecule $G\beta\gamma$ inhibitors suppressed fMLP-stimulated Rac activation, superoxide production, and PI3-kinase activation in differentiated HL60 cells. These compounds also blocked fMLP-dependent chemotaxis in HL60 cells and primary human neutrophils. Systemic administration inhibited paw edema and neutrophil infiltration in a mouse carrageenan-induced paw edema model. Overall the data demonstrate that targeting $G\beta\gamma$ -regulation may be an effective anti-inflammation strategy.

Introduction

Chemoattractant-mediated recruitment of leukocytes is responsible for many of the deleterious effects of chronic inflammatory diseases. Many chemoattractants activate G protein-coupled receptors (GPCRs) coupled to the G_i family of heterotrimeric G proteins in leukocytes. Heterotrimeric G proteins are composed of $G\alpha$, $G\beta$, and $G\gamma$ subunits. Ligand binding to receptors catalyzes the exchange of tightly bound GDP for GTP on the $G\alpha$ subunit, liberating it from the $G\beta\gamma$ subunits. Dissociation of the $G\alpha$ and $G\beta\gamma$ subunits can allow each to directly bind to downstream effector proteins (Oldham and Hamm, 2006; Gilman, 1987). It is the free $G\beta\gamma$ subunits released from G_i heterotrimers upon chemoattractant receptor activation that initiate critical signaling pathways to direct chemoattractant-dependent neutrophil functions including chemotaxis and superoxide production (Neptune and Bourne, 1997).

Key direct targets of $G\beta\gamma$ subunit binding and activation in neutrophils are Phosphoinositide 3-kinase γ (PI3-kinase γ) (Stephens *et al.*, 1997; Stephens *et al.*, 1994; Stoyanov *et al.*, 1995), Phospholipase C β (PLC β) (Wu *et al.*, 2000), and P-Rex (Welch *et al.*, 2002). PI3-kinase γ has been noted to be a central mediator of chemotaxis and plays a pivotal role in leukocyte recruitment to inflamed tissues (Li *et al.*, 2000; Camps *et al.*, 2005; Hirsch *et al.*, 2000). PIP₃ produced by PI3-kinase γ catalytic activity is critical to the development of cell polarity which is necessary for chemokine-mediated cell motility and directional sensing (Wu *et al.*, 2000). PI3-kinase γ -deficient neutrophils have impaired responses to various chemoattractants, including diminished chemotaxis (Li *et al.*, 2000; Hirsch *et al.*, 2000) and respiratory burst (Li *et al.*,

MOL #41780

2000;Sasaki *et al.*, 2000), in response to GPCR activation. Small molecule inhibitors of PI3-kinase γ catalytic activity have been demonstrated to suppress joint inflammation in mouse models of inflammation (Barber *et al.*, 2005;Camps *et al.*, 2005). Critical to the success of an approach that targets PI3-kinase γ activity as a therapeutic anti-inflammatory approach is development of selective inhibitors that do not target other PI3-kinase isoforms since these enzymes are critically involved in multiple aspects of mammalian cell function (Ruckle *et al.*, 2006).

Here, we demonstrate a novel strategy to inhibit chemoattractant-dependent chemotaxis and inflammation using recently identified compounds that block G β γ -interactions with effectors including PI3-kinase γ by binding to a protein-protein interaction “hot spot” on the G β subunit (Bonacci *et al.*, 2006). We show that these compounds block fMLP-dependent PI3-kinase γ activation, Rac1 activation, superoxide production and neutrophil migration *in vitro*. Further, when administered *in vivo*, neutrophil-dependent inflammation is inhibited demonstrating that suppressing key G β γ -dependent signaling functions with small molecules has significant anti-inflammatory potential.

Materials and Methods

Small molecules. Compounds for this study were kindly provided by the NCI repository except when indicated otherwise. Compound abbreviations are as follows: M119 (NSC119910), M119B (NSC119892). Gallein, fluorescein, and wortmannin were obtained from Sigma Aldrich (St. Louis, MO).

Competition ELISA and structure activity relationships. Binding of small molecules to $G\beta_1\gamma_2$ was assessed by competition with phage displaying the SIGK peptide as described (Scott *et al.*, 2001; Bonacci *et al.*, 2006). Briefly, $G\beta_1\gamma_2$ (25 nM), with biotin incorporated via an N-terminal acceptor peptide on $G\beta_1$, was immobilized in a 96-well plate coated with streptavidin. Compounds/DMSO and 0.1×10^{10} phage were added simultaneously and subsequently incubated for 1 h at room temperature. Plates were then washed with 1X TBS/0.5% Tween 20 and incubated with anti-M13, horseradish peroxidase conjugated, antibody (Amersham Biosciences; Piscataway, NJ). Phage binding was determined by monitoring A_{405} upon addition of 2,2'-Azino-bis(3-ethylbenzothiazoline-6-sulfonic acid (Sigma Aldrich).

Surface plasmon resonance. Direct binding of “hot spot” binding small molecules was assessed using the Reichert SR7000 Surface Plasmon Resonance dual chamber instrument equipped with an autosampler (Reichert; Depew, NY). To activate the sensor chip surface a mixture of 0.1M 1-ethyl-3-(3-dimethylaminopropyl) carbodiimide hydrochloride (EDC) and 0.05M N-hydroxysuccinimide (NHS) was injected (flow rate 5

MOL #41780

$\mu\text{L}/\text{min}$) over the sensor surface. Streptavidin ($100 \mu\text{g}/\text{mL}$; prepared in 20 mM sodium acetate buffer pH 5.5) was coupled to the sensor chip surface followed by quenching the remaining activated carboxyl groups with 1 M ethanolamine (pH 8.5). $\text{bG}\beta_1\gamma_2$ was conjugated to the streptavidin coated chip in running buffer (50 mM Hepes, pH 7.6, 1 mM EDTA, 100 mM NaCl, 0.1% $\text{C}_{12}\text{E}_{10}$, 1 mM DTT) to achieve $2000 \mu\text{RIUs}$. A second reference cell was treated similarly, but $\text{bG}\beta_1\gamma_2$ was excluded. Direct binding of small molecules was tested out at room temperature with a flow rate of $75 \mu\text{L}/\text{min}$ flow rate. Compounds were prepared in running buffer and injected for 10 minutes followed by a dissociation phase of 10 minutes. The obtained sensorgrams were corrected for non-specific background by running the same experiment in series over an identical sensor surface with immobilized streptavidin, blocked with biotin, without $\text{bG}\beta\gamma$. Binding rates and constants were independent of flow rate over a wide range and did not fit mass transport limited models indicating that mass transport was not limiting association or dissociation rates. Best fit kinetic parameters were determined using kinetic titration model and ClampXP v3.5 that accounts for incomplete dissociation between injections (Karlsson *et al.*, 2006).

GFP-PH-Akt translocation in differentiated HL60 cells. HL60 cells stably overexpressing GFP-PH-Akt (Servant *et al.*, 2000) were maintained and differentiated as previously described (Bonacci *et al.*, 2006). Cells (0.2×10^6 cells/ml) were differentiated by incubation with 1.2% DMSO for 5 days. Cells were washed with serum-free RPMI 1640 (Invitrogen; Carlsbad, CA). Two hundred thousand cells ($100 \mu\text{l}$) were transferred to a 1.8 ml Beckman ultracentrifuge tube. Cells were pretreated with DMSO or

MOL #41780

compounds for 10 min. at room temperature and stimulated with 250 nM fMLP (Sigma Aldrich) for 2 min. at 37 °C, snap-frozen in liquid nitrogen, and thawed in the presence of 100 μ l 2X lysis buffer (100 mM HEPES (pH 8.0), 6 mM MgCl₂, 0.2 mM EDTA, 200 mM NaCl, 100 μ M Na₃VO₄, and protease inhibitors). Membranes were harvested by centrifugation 100,000 x g for 20 min. following four freeze-thaw cycles. All treatments contained the same final concentration of DMSO. Pellets were washed once with 100 μ l lysis buffer (50 mM HEPES (pH 8.0), 3 mM MgCl₂, 0.1 mM EDTA, 100 mM NaCl, 50 μ M Na₃VO₄, and protease inhibitors), pelleted as above and boiled in 2X sample loading buffer. Samples were resolved by 12% SDS-PAGE, transferred to nitrocellulose and probed with anti-GFP antibody (1:1000; Roche) followed by incubation with goat anti-mouse HRP conjugated secondary antibody (1:5000, BioRad; Hercules, CA). Chemiluminescence was analyzed using a CCD camera in a UVP Epi-Chem II Darkroom imaging system. All samples had background subtracted and were normalized to the fMLP-induced signal set at 100 %.

Cell motility analysis. Chemotaxis was assayed using a Boyden chamber (Neuro Probe, Gaithersburg, MD) using 3 μ m polyvinylpyrrolidone-free polycarbonate filters (Neuro Probe). HL60 cells (differentiated for 4 days) were washed with and resuspended in HBSS containing 1% BSA to a final concentration of 1 x 10⁶ cells/ml. Primary human neutrophils were washed and resuspended in NaCl buffer (140 mM NaCl, 4 mM KCl, 10 mM D-glucose, 10 mM HEPES, pH 7.4, 1 mM MgCl₂, 1 mM CaCl₂) to a final concentration of 1 x 10⁶ cells/ml. Chemoattractant (1 μ M GM-CSF, 10 nM IL-8 or 250 nM fMLP; Sigma Aldrich) was added to the bottom chamber in HBSS containing 1%

MOL #41780

BSA. Cell suspensions (0.2×10^6 cells/well) were added to the top wells of the Boyden chamber and allowed to migrate for 1 h at 37 °C. When applicable, cell suspensions were pre-incubated for 10 min. with small molecule inhibitors (in DMSO) at the indicated concentrations and the bottom chamber was adjusted to the same concentration of small molecule. All treatments contained the same final concentration of DMSO. Filters were processed according to the manufacture's recommendations and stained using DifQuik (VWR Scientific; West Chester, PA). Chemotactic HL60 cells were scored by counting 3 microscope fields and subtracting the number of cells from -fMLP wells as background. All samples had background subtracted and were normalized to the fMLP-induced signal set at 100 %. For all the small molecules, effects of the compounds on chemokinesis was analyzed by measuring chemotaxis in the presence of 250 nM fMLP in both the upper and lower chambers of the Boyden Chamber and measuring changes in transwell migration. Unless otherwise indicated none of the compounds had effects on chemokinesis.

Measurement of superoxide production. The nitrotetrazolium blue (NBT) method was used to assess the effects of Gβγ inhibitors on NADPH oxidase activity. HL60 cells (differentiated for 4 days) were washed with and resuspended in HBSS containing calcium and magnesium (Cellgro; Herndon VA) to a final concentration of 2×10^6 cells/ml. Cells (1×10^6 /rxn) were pretreated with 10 μM Gβγ inhibitor compound (in DMSO) or 100 nM wortmanin (Sigma Aldrich) for 10 min. at 37 °C prior to the addition of NBT (25 μl of 10 mg/ml in methanol) and then incubated for an additional 5 min. at 37 °C. All treatments contained the same final concentration of DMSO. Cells were then

MOL #41780

activated with either 250 nM fMLP (Sigma Aldrich) or PMA (Sigma Aldrich) for 30 min. in a 37 °C water bath. Reactions were stopped by the addition of 500 µl of 1.2 N HCl and cells collected by centrifugation at 12,000 x g for 5 minutes. Cell pellets were then resuspended in 200 µl DMSO, transferred to a 96-well plate and absorbance measured at 540 nM. All treatments and controls contained the same concentration of DMSO. All samples had background subtracted and were normalized to the fMLP-induced signal set at 100 %.

Evaluation of Rac-1 activation. HL60 cells (differentiated for 4 days) were washed with and resuspended in NaCl buffer to a final concentration of 20×10^6 cells/ml. Cells (10×10^6 /rxn) were pretreated with 10 µM Gβγ inhibitor (in DMSO) for 10 min. prior to challenge with 1 µM fMLP for 90 seconds in a 37 °C water bath and then immediately transferred to an ice-water bath. Cells were recovered by centrifugation at 500 x g and washed two times with ice-cold TBS, pH 7.4. The Rac1 activation assay kit (Upstate Cell Signaling Solutions; Temecula, CA) was used to prepare cell extracts and evaluate Rac1 activation according to the manufactures' instructions. Affinity purified GTP-Rac1 was resolved by 15% SDS-PAGE, transferred to nitrocellulose, probed with anti-Rac1 monoclonal antibody followed by detection with HRP-conjugated secondary antibody in accordance with the manufactures' recommendations. Chemiluminescence was analyzed using a CCD camera in a UVP Epi-Chem II Darkroom imaging system. Results were expressed as percent fMLP-stimulated GTP Rac1 normalized to total Rac1 with the background subtracted.

MOL #41780

Carrageenan-induced paw edema and neutrophil abundance. Male Swiss Webster mice (35-40 g BW; Taconic Farms, Germantown, NY) were randomized and acclimated for one week in a 12 h light/dark cycle. Food and water were provided *ad libitum*. Animals were labeled with unique identifiers on their tails using indelible marker. One hour prior to challenge with carrageenan, mice were administered compounds (dissolved in PBS) or vehicle (PBS) either by intraperitoneal (300 μ L with 27 1/2 gauge needle) injection or by oral gavage (100 μ l with 1 1/2" long, steel ball-tipped feeding needle; Popper and Sons, New Hyde Park, NY). Indomethacin, 2.5 mg/kg, stock solution was prepared in methanol and diluted into PBS (Cellgro), small molecule inhibitor (concentration as indicated in appropriate figure legend was prepared in PBS. Mice were anesthetized by intraperitoneal injection with ketamine hydrochloride (175 mg/kg) and xylazine (7 mg/kg) using a 26 gauge needle. Mice were tested for pain reflex to ensure sedation and then injected subcutaneously into the plantar region of the hind paw with 25 μ l of 2% carrageenan using a precision engineered 5/8" long 25 gauge Hamilton syringe (hypodermic needle (Hamilton Co., Reno, NV). Carrageenan (CarboMer, Inc., San Diego, CA) was suspended in PBS at 50 °C for 10 min. with stirring the night before experimentation. The contralateral paw was injected with vehicle as control. Mice were then transferred to bedded cages to minimize pain associated with the carrageenan injections. Dorsal-plantar swelling was measured using an electronic digital caliper (+/- 0.03 mm; VWR Scientific) at time zero and every 2 h thereafter. To ensure measuring and injection consistency, the dorsal and plantar surface of the test paw and contralateral paws of each animal were marked with indelible marker. Each paw was measured two times at each time point and averaged. At the conclusion of the experiment, animals

MOL #41780

were euthanized in accordance with the University of Rochester and American Veterinary Medical Association standards by carbon dioxide narcosis and cervical dislocation. Paw edema was determined by subtracting the thickness of the contralateral paw from that of the carrageenan injected paw at each time point.

Paws were amputated 2 h post carrageenan injection to determine the number of neutrophils present in the edematous fluid. Paws were transferred to pre-tared Eppendorf tubes and the exudates were collected by centrifugation for 2 minutes. The paws were removed and the tubes re-weighed to determine the mass of the exudates which was then converted to volume. To remove erythrocytes by hypertonic lysis, the exudate was resuspended in 250 μ l 1X PBS to which 50 μ l of water was added. At the conclusion of a 30 second incubation 75 μ l of 4.5X PBS was added to return the solution to normal salt levels. The number of neutrophils present was determined by manual counting.

Isolation of primary human neutrophils. Human blood obtained by venous puncture from consenting, healthy adult donors, in accordance with University of Rochester standards, and collected in sterile vacutubes containing sodium heparin (BD Biosciences; San Jose, CA). Neutrophils were layered over PolymorphprepT11 (Accurate Chemical and Scientific Co.; Westbury, NY) and isolated by centrifugation (470 x g for 50 min. at room temperature). Trace erythrocytes were removed by hypertonic treatment followed by centrifugation. Isolated neutrophils were stored in BSS solution (146 mM NaCl, 5 mM KCl, 5.5 mM D-Glucose, 10 mM HEPES, 1 μ M CaCl₂, 1 mM MgSO₄) at pH 7.4.

MOL #41780

Data analysis. Ligand competition curves were determined by non-linear regression using Prism software (GraphPad Software, Inc.). Statistical significance was evaluated by one-way analysis of variance and Bonferroni's Multiple Comparison Test. Statistical significance was defined as *P < 0.05, **P < 0.01, ***P < 0.001.

Results

Characterization of Novel Compound Binding to Gβγ.

Previous studies identified multiple compounds that blocked effector binding to Gβγ. A lead compound, M119, inhibited Gβγ-dependent PI3-kinase γ and PLC β activation *in vitro* and blocked chemoattractant/PI3-kinase-dependent GFP-PH-Akt translocation to membranes as well as Ca²⁺ release (Bonacci *et al.*, 2006). We identified a related compound, gallein, which differs from M119 by the substitution of a benzene carboxylic acid for cyclohexane carboxylic acid at the 9 position of the core xanthene (Figure 1A). Gallein is commercially available at high purity as a single isomer and in quantities necessary for *in vivo* analysis so the Gβγ binding properties of gallein were compared with M119. Gallein effectively competed for binding of SIGK peptide to Gβγ in a phage ELISA assay with an IC₅₀ comparable to that of M119 (Figure 1B). We have previously shown that compounds that block peptide binding in this assay are effective competitors of many Gβγ protein-protein interactions.

To determine direct binding equilibrium and kinetic constants for gallein binding to Gβγ, surface plasmon resonance (SPR) measurements were performed with streptavidin immobilized biotinylated Gβ₁γ₂. Binding and dissociation of gallein was monitored as a function of concentration and time. Data were fit to one site association and dissociation models to calculate association and dissociation rate constants from which affinity constants were derived (Fig. 1C, Table 1). Based on the SPR analysis, gallein bound to Gβ₁γ₂ (Figure 1C) with a K_d value of approximately 400 nM (Table 1),

MOL #41780

in relatively close agreement with the IC_{50} of 200 nM observed in the competition ELISA assay. The control compound, fluorescein, which did compete for SIGK binding in the competition ELISA, did not have detectable binding by SPR (Table 1). Interestingly, binding and dissociation rates for gallein were relatively slow (Figure 1C). These data confirm that gallein binds directly to $G\beta\gamma$ and resulting effects on competition for effector binding are likely to result from direct binding to $G\beta\gamma$ with high affinity. Based on these data, gallein would be predicted to have similar effects to M119 when tested in *in vitro* and *in vivo* assays.

Inhibition of G protein dependent chemotactic peptide signaling with small molecules.

A key molecule involved in chemotactic peptide signaling is PI3-kinase γ . To determine if gallein, like M119, modulates the receptor-dependent activation of PI3-kinase, HL60 cells expressing GFP-PH-Akt were pre-treated with compound and challenged with fMLP. Gallein inhibited fMLP-dependent GFP-PH-Akt translocation in differentiated HL60 cells with an efficacy comparable to M119 (Figure 2A).

Activation of Rac in neutrophils is critical for fMLP-dependent activation of NADPH-oxidase and subsequent superoxide production and is dependent on $G\beta\gamma$ and PIP_3 dependent activation of the Rac-specific exchange factor P-Rex. Other previous work showed that M119 inhibited P-Rex1 activation by fMLP suggesting the compounds could inhibit Rac activation (Zhao *et al.*, 2007). We determined if $G\beta\gamma$ -binding compounds would inhibit receptor-dependent activation of Rac1. Rac1GTP levels were measured in cytosolic extracts of HL60 cells that had been pretreated with compounds

MOL #41780

before stimulation with fMLP. M119 and gallein inhibited fMLP-induced Rac1 activation in differentiated HL60 cells, whereas, the negative control compound M119B had little effect (Figure 2B).

Gβγ inhibitors block fMLP-dependent superoxide production and neutrophil chemotaxis.

The ability of these small molecules to block fMLP-induced chemotaxis and superoxide production was assessed to determine if the compounds could block relevant cellular functions downstream of PI3-kinase γ and Rac. Both of these functions are critical to the inflammatory process and inhibition of both processes could contribute to anti-inflammatory effects of G $\beta\gamma$ inhibitors.

M119 and Gallein both significantly inhibited fMLP-dependent superoxide production. Control compounds M119B and fluorescein did not significantly affect this response (Fig 2C). Wortmannin also blocked fMLP-dependent superoxide production indicating the pathway was a PI3kinase dependent pathway. We also examined PMA dependent superoxide production, a process not dependent on G $\beta\gamma$. PMA-dependent superoxide production was not inhibited by any of the G $\beta\gamma$ binding compounds or controls (Fig 2D) indicating that the compounds specifically inhibited the G $\beta\gamma$ -dependent pathway to superoxide production.

fMLP-dependent chemotaxis was assessed in a Boyden Chamber. M119 and gallein inhibited fMLP-induced chemotaxis in differentiated HL60 cells with similar efficacy (Figure 3A). Neither M119 nor gallein had any effects on chemokinesis

MOL #41780

measured in the transwell assay with fMLP in both the upper and lower chambers (data not shown). To support the idea that the mode of action of these compounds is dependent on G $\beta\gamma$ heterodimers liberated from G α_i -coupled chemokine receptors, cells were challenged with granulocyte-macrophage-colony stimulating factor (GM-CSF). GM-CSF-induced chemotaxis is partly dependent on PI3-kinase activity in human neutrophils, but is independent of G $\beta\gamma$ -stimulation of PI3-kinase (Gomez-Cambronero *et al.*, 2003). If the small molecules were acting directly on PI3-kinase or by a nonspecific mechanism they would be expected to block GM-CSF-induced chemotaxis. Neither M119 nor gallein blocked GM-CSF induced chemotaxis in differentiated HL60 cells (Figure 3B). These data demonstrate two key points: 1) The general chemotaxis machinery in HL60 cells is not affected by these compounds and 2) the compounds selectively inhibited GPCR dependent chemotaxis, consistent with inhibition of G $\beta\gamma$ signaling.

The inhibitory properties of these compounds in potentially more clinically relevant isolated primary human neutrophils were also evaluated. Again, both M119 and gallein significantly inhibited fMLP-induced chemotaxis (Figure 3C). Wortmannin, a general PI3-kinase inhibitor (Okada *et al.*, 1994), also blocked chemotaxis (Figure 3C). Conversely, M119B, only binds weakly to the G $\beta\gamma$ “hot spot” (Table 1., (Bonacci *et al.*, 2006)), had no affect on cell motility (Figure 3C) suggesting that the observed effects on chemotaxis are dependent on small molecule binding to the G $\beta\gamma$ “hot spot”. IL-8 regulated chemotaxis was also blocked by M119 and gallein (Figure 3C) extending our findings to other G $_i$ coupled chemoattractants and supporting the idea that the mechanism

MOL #41780

of action of these compounds is to inhibit G $\beta\gamma$ subunit signaling downstream of chemoattractant/chemokine receptors.

To assess the potency of gallein for inhibition of chemotaxis, primary human neutrophils were treated with a range of concentrations and assayed for fMLP-dependent chemotaxis. Gallein blocked fMLP-dependent chemotaxis with an IC₅₀ of approximately 5 μ M (Figure 3D). Thus small molecules that bind to G $\beta\gamma$ and block G $\beta\gamma$ -dependent PI3-kinase γ regulation *in vitro* and in HL60 cells, potently inhibit GPCR dependent neutrophil chemotaxis with an IC₅₀ comparable to what has been published for direct PI3-kinase catalytic inhibitors on chemokine-dependent monocyte chemotaxis (Camps *et al.*, 2005).

Gallein attenuates inflammation and neutrophil recruitment in vivo.

Inhibition of chemoattractant-dependent chemotaxis of neutrophils would be predicted to inhibit neutrophil-dependent inflammation based on data from PI3-kinase γ knock out mice (Li *et al.*, 2000;Hirsch *et al.*, 2000). To assess the *in vivo* efficacy of G $\beta\gamma$ -binding small molecules in blocking neutrophil chemotaxis we tested gallein in the carrageenan paw edema model. Carrageenan, when injected into the glabrous tissue of the hind paw, leads to rapid acute inflammation characterized by infiltration of neutrophils (Siqueira-Junior *et al.*, 2003). Gallein or vehicle control was delivered by intraperitoneal injection 1 h prior to injection of carrageenan into the paw. Peak paw edema was observed 2 h post carrageenan injection (Figure 4A). Indomethacin, a nonselective nonsteroidal anti-inflammatory drug (NSAID) that inhibits cyclooxygenases

MOL #41780

1 and 2 (Siqueira-Junior *et al.*, 2003), is the drug-of-choice for comparative *in vivo* efficacy studies. Pretreatment with indomethacin sharply reduced paw edema. Significantly, prophylactic administration of 100 mg/kg gallein reduced paw edema to levels comparable to that of indomethacin. Injection with gallein in the absence of carrageenan had no effect on paw thickness (data not shown). Additional experimentation determined that the ED₅₀ value of gallein for inhibiting paw edema to be approximately 20 mg/kg (Figure 4B). Acute phase inflammation, as seen in the carrageenan-induced paw edema model, is characterized by neutrophil infiltration (Siqueira-Junior *et al.*, 2003; Posadas *et al.*, 2004). To confirm that neutrophil infiltration was inhibited, the number of neutrophils in paw exudates was quantified. Pretreatment with 100 mg/kg gallein reduced the number of neutrophils in the edematous fluid by approximately half to levels comparable to that seen with indomethacin (Figure 4C). These data correlated well with the actual volume of exudate fluid. Pretreatment with indomethacin and gallein also reduced exudate volume by approximately 75% (Figure 4D).

Oral administration of gallein (30 mg/kg) in mice 1 h prior to carrageenan challenge also significantly reduced paw swelling by 40% comparable to that of indomethacin (Figure 5). These data demonstrate that gallein is absorbed into systemic circulation, is bioavailable and systemically impairs neutrophil recruitment. To support the conclusion that the observed reduction in paw swelling was G β γ dependent we tested the M119B-like compound fluorescein under identical experimental conditions. Fluorescein differs from M119B only by the substitution of an aromatic benzene ring for

MOL #41780

a cyclohexane at the 9 position of the core xanthene (Figure 1A) and binds $G\beta\gamma$ very weakly if at all (Table 1). Fluorescein did not reduce paw swelling under identical experimental conditions (Figure 5) and indicate that the observed reduction in paw swelling and neutrophil infiltration correlates with the ability of the small molecules to bind to $G\beta\gamma$.

Discussion

Here we present a novel strategy for treatment of inflammation that targets interactions between G protein $\beta\gamma$ subunits and effectors that are critical for neutrophil migration in response to activation of chemoattractant receptors. $G\beta\gamma$ -responsive PI3-kinase γ production of PI 3,4,5 P_3 is critical to neutrophil functions, including superoxide production, chemotaxis, and cellular polarization (Li *et al.*, 2000;Hirsch *et al.*, 2000). We have shown that $G\beta\gamma$ binding small molecules inhibit interactions between $G\beta\gamma$ and PI3-kinase γ . These same molecules block PI3-kinase and Rac1 activation in HL60 cells, chemoattractant-dependent superoxide production and chemotaxis in differentiated HL60 cells. These findings were extended to inhibition of chemoattractant-dependent chemotaxis in primary human neutrophils and ultimately neutrophil-dependent inflammation *in vivo*.

PI3-kinases play diverse roles in normal cellular physiology including cell motility and survival (Cantley, 2002). Camps and colleagues identified and characterized small molecule inhibitors of PI3-kinase γ that are competitive with ATP (Camps *et al.*, 2005). These small molecules were efficacious in mouse models of rheumatoid arthritis and systemic lupus providing further rationale for pharmacological targeting of the pathway as therapeutic strategy (Camps *et al.*, 2005;Barber *et al.*, 2005). However, a concern with inhibitors of this class is that since many kinases of the same family have significant homology and there may be difficulty in developing inhibitors that are selective for PI3-kinase γ , although some progress has been made in this area (Ruckle *et al.*, 2006). The strategy presented here selects for a single isoform of the PI3-kinase

MOL #41780

family since PI3-kinase γ is the only PI3-kinase isoform that uses a $G_i\beta\gamma$ -dependent as a major mechanism for regulation (Stephens *et al.*, 1997; Stephens *et al.*, 1994; Hirsch *et al.*, 2000).

Compounds like M119 and gallein also inhibit interactions between $G_i\beta\gamma$ and other targets that are critical for chemoattractant-dependent directed migration or ROS production by neutrophils or other monocytes. For example, M119 blocks membrane translocation of P-Rex, a PIP_3 and $G_i\beta\gamma$ regulated Rac2 exchange factor, in human neutrophils which could be in part due to directly blocking P-Rex binding to $G_i\beta\gamma$ in addition to blocking PIP_3 production by PI3-kinase (Zhao *et al.*, 2007). It has recently been shown that Ras is required for full PI3-kinase γ activation in neutrophils (Suire *et al.*, 2006). It is possible that the inhibitors block $G_i\beta\gamma$ -dependent activation of Ras and in part act to block PI3-kinase γ activation in cells indirectly through inhibition of Ras activation. In Dictyostelium both PI3-kinase and PLA_2 activities downstream of G protein activation are important for chemotaxis (Chen *et al.*, 2007). Other studies have shown chemoattractant dependent chemotaxis becomes PI3-kinase independent under certain conditions (Ferguson *et al.*, 2007). Thus, a broad spectrum $G_i\beta\gamma$ inhibitor could be more effective, in some cases, than selective PI3-kinase γ inhibitors because they can block other $G_i\beta\gamma$ interactions besides PI3-kinase- γ , a property that could contribute to therapeutic efficacy. Nevertheless, because of the wide roles of $G_i\beta\gamma$ in regulation of cell physiology development of $G_i\beta\gamma$ binding small molecules that are more selective for PI3-kinase γ inhibition relative to other $G_i\beta\gamma$ -dependent pathways is an important direction.

MOL #41780

Inflammation is a central mediator of many human conditions, including atherosclerosis, allergic reactions, psoriasis, virus-induced myocarditis, ischemia-reperfusion injury, and rheumatoid arthritis. The inflammatory process involves complex signaling cascades partly coordinated by chemokines, which recruit leukocytes, including large numbers of neutrophils, to sites of inflammation (Wu *et al.*, 2000). Targeting chemokines with antibodies or binding proteins as well as targeting chemokine receptors has been attempted as a therapeutic strategy (Barnes *et al.*, 1998;Gong *et al.*, 1997;Halloran *et al.*, 1999;Matthys *et al.*, 2001;Ogata *et al.*, 1997;Plater-Zyberk *et al.*, 1997;Podolin *et al.*, 2002;Yang *et al.*, 2002) However, the overwhelming complexity of these signaling molecules (multiple chemokines, chemokine receptors, and redundancy) is a significant hurdle. Polychemokine (Carter, 2002) or combinations of different chemokine (al Mughales *et al.*, 1996) antagonists have been suggested, but there may be chemokines that act as an agonist at one receptor and an antagonist at another (Xanthou *et al.*, 2003). Despite this complexity, these chemokine receptors and ligands represent a tantalizing therapeutic target because of their integral role in the inflammatory process. Targeting PI3-kinase γ has been suggested as strategy for blocking a common signal downstream of chemokine receptors (Camps *et al.*, 2005;Ruckle *et al.*, 2006). The data presented here indicates that targeting $G\beta\gamma$ could also circumvent the redundancy of the chemokine system and may offer some advantages to direct targeting of PI3-kinase γ .

MOL #41780

Acknowledgements:

The authors would like to thank the Developmental Therapeutics Program at the NCI/NIH for providing small molecules used in this study, H. Bourne for providing HL60 cells stably overexpressing GFP-PH-Akt, R. Waugh for purifying human neutrophils and J. Bidlack and B. Fulton for valuable discussions.

MOL #41780

References

- al Mughales J, Blyth T H, Hunter J A and Wilkinson P C (1996) The Chemoattractant Activity of Rheumatoid Synovial Fluid for Human Lymphocytes Is Due to Multiple Cytokines. *Clin Exp Immunol* **106**: 230-236.
- Barber DF, Bartolome A, Hernandez C, Flores J M, Redondo C, Fernandez-Arias C, Camps M, Ruckle T, Schwarz M K, Rodriguez S, Martinez A, Balomenos D, Rommel C and Carrera A C (2005) PI3K γ Inhibition Blocks Glomerulonephritis and Extends Lifespan in a Mouse Model of Systemic Lupus. *Nat Med* **11**: 933-935.
- Barnes DA, Tse J, Kaufhold M, Owen M, Hesselgesser J, Strieter R, Horuk R and Daniel Perez H (1998) Polyclonal Antibody Directed Against Human RANTES Ameliorates Disease in the Lewis Rat Adjuvant-Induced Arthritis Model. *J Clin Invest* **101**: 2910-2919.
- Bonacci TM, Mathews J L, Yuan C, Lehmann D M, Malik S, Wu D, Font J L, Bidlack J M and Smrcka A V (2006) Differential Targeting of G $\beta\gamma$ -Subunit Signaling With Small Molecules. *Science* **312**: 443-446.
- Camps M, Ruckle T, Ji H, Ardisson V, Rintelen F, Shaw J, Ferrandi C, Chabert C, Gillieron C, Francon B, Martin T, Gretener D, Perrin D, Leroy D, Vitte P A, Hirsch E, Wymann M P, Cirillo R, Schwarz M K and Rommel C (2005) Blockade of PI3K γ Suppresses Joint Inflammation and Damage in Mouse Models of Rheumatoid Arthritis. *Nat Med* **11**: 936-943.
- Cantley LC (2002) The Phosphoinositide 3-Kinase Pathway. *Science* **296**: 1655-1657.
- Carter PH (2002) Chemokine Receptor Antagonism As an Approach to Anti-Inflammatory Therapy: 'Just Right' or Plain Wrong? *Current Opinion in Chemical Biology* **6**: 510-525.
- Chen L, Iijima M, Tang M, Landree M A, Huang Y E, Xiong Y, Iglesias P A and Devreotes P N (2007) PLA2 and PI3K/PTEN Pathways Act in Parallel to Mediate Chemotaxis. *Developmental Cell* **12**: 603-614.
- Ferguson GJ, Milne L, Kulkarni S, Sasaki T, Walker S, Andrews S, Crabbe T, Finan P, Jones G, Jackson S, Camps M, Rommel C, Wymann M, Hirsch E, Hawkins P and Stephens L (2007) PI(3)K γ Has an Important Context-Dependent Role in Neutrophil Chemokinesis. *Nat Cell Biol* **9**: 86-91.
- Gilman AG (1987) G Proteins: Transducers of Receptor-Generated Signals. *Ann Rev Biochem* **56**: 615-649.

MOL #41780

- Gomez-Cambronero J, Horn J, Paul C C and Baumann M A (2003) Granulocyte-Macrophage Colony-Stimulating Factor Is a Chemoattractant Cytokine for Human Neutrophils: Involvement of the Ribosomal P70 S6 Kinase Signaling Pathway. *J Immunol* **171**: 6846-6855.
- Gong JH, Ratkay L G, Waterfield J D and Clark-Lewis I (1997) An Antagonist of Monocyte Chemoattractant Protein 1 (MCP-1) Inhibits Arthritis in the MRL-Lpr Mouse Model. *J Exp Med* **186**: 131-137.
- Halloran MM, Woods J M, Strieter R M, Szekanecz Z, Volin M V, Hosaka S, Haines G K, III, Kunkel S L, Burdick M D, Walz A and Koch A E (1999) The Role of an Epithelial Neutrophil-Activating Peptide-78-Like Protein in Rat Adjuvant-Induced Arthritis. *J Immunol* **162**: 7492-7500.
- Hirsch E, Katanaev V L, Garlanda C, Azzolino O, Pirola L, Silengo L, Sozzani S, Mantovani A, Altruda F and Wymann M P (2000) Central Role for G Protein-Coupled Phosphoinositide 3-Kinase γ in Inflammation. *Science* **287**: 1049-1053.
- Karlsson R, Katsamba P S, Nordin H, Pol E and Myszka D G (2006) Analyzing a Kinetic Titration Series Using Affinity Biosensors. *Analytical Biochemistry* **349**: 136-147.
- Li Z, Jiang H, Xie W, Zhang Z, Smrcka A V and Wu D (2000) Roles of PLC β -2 and β -3 and PI3K γ in Chemoattractant-Mediated Signal Transduction. *Science* **287**: 1046-1049.
- Matthys P, Hatse S, Vermeire K, Wuyts A, Bridger G, Henson G W, De Clercq E, Billiau A and Schols D (2001) AMD3100, a Potent and Specific Antagonist of the Stromal Cell-Derived Factor-1 Chemokine Receptor CXCR4, Inhibits Autoimmune Joint Inflammation in IFN- γ Receptor-Deficient Mice. *J Immunol* **167**: 4686-4692.
- Neptune ER and Bourne H R (1997) Receptors Induce Chemotaxis by Releasing the β Subunit of Gi, Not by Activating Gq or Gs. *Proc Natl Acad Sci U S A* **94**: 14489-14494.
- Ogata H, Takeya M, Yoshimura T, Takagi K and Takahashi K (1997) The Role of Monocyte Chemoattractant Protein-1 (MCP-1) in the Pathogenesis of Collagen-Induced Arthritis in Rats. *J Pathol* **182**: 106-114.
- Okada T, Sakuma L, Fukui Y, Hazeki O and Ui M (1994) Blockage of Chemotactic Peptide-Induced Stimulation of Neutrophils by Wortmannin As a Result of Selective Inhibition of Phosphatidylinositol 3-Kinase. *J Biol Chem* **269**: 3563-3567.
- Oldham WM and Hamm H E (2006) Structural Basis of Function in Heterotrimeric G Proteins. *Q Rev Biophys* **39**: 117-166.
- Plater-Zyberk C, Hoogewerf A J, Proudfoot A E I, Power C A and Wells T N C (1997) Effect of a CC Chemokine Receptor Antagonist on Collagen Induced Arthritis in DBA/1 Mice. *Immunology Letters* **57**: 117-120.

MOL #41780

Podolin PL, Bolognese B J, Foley J J, Schmidt D B, Buckley P T, Widdowson K L, Jin Q, White J R, Lee J M, Goodman R B, Hagen T R, Kajikawa O, Marshall L A, Hay D W P and Sarau H M (2002) A Potent and Selective Nonpeptide Antagonist of CXCR2 Inhibits Acute and Chronic Models of Arthritis in the Rabbit. *J Immunol* **169**: 6435-6444.

Posadas I, Bucci M, Roviezzo F, Rossi A, Parente L, Sautebin L and Cirino G (2004) Carrageenan-Induced Mouse Paw Oedema Is Biphasic, Age-Weight Dependent and Displays Differential Nitric Oxide Cyclooxygenase-2 Expression. *Br J Pharmacol* **142**: 331-338.

Ruckle T, Schwarz M K and Rommel C (2006) PI3K γ Inhibition: Towards an 'Aspirin of the 21st Century'? *Nat Rev Drug Discov* **5**: 903-918.

Sasaki T, Irie-Sasaki J, Jones R G, Oliveira-dos-Santos A J, Stanford W L, Bolon B, Wakeham A, Itie A, Bouchard D, Kozieradzki I, Joza N, Mak T W, Ohashi P S, Suzuki A and Penninger J M (2000) Function of PI3K in Thymocyte Development, T Cell Activation, and Neutrophil Migration. *Science* **287**: 1040-1046.

Scott JK, Huang S F, Gangadhar B P, Samoriski G M, Clapp P, Gross R A, Taussig R and Smrcka A V (2001) Evidence That a Protein-Protein Interaction 'Hot Spot' on Heterotrimeric G Protein B γ Subunits Is Used for Recognition of a Subclass of Effectors. *EMBO J* **20**: 767-776.

Servant G, Weiner O D, Hezmark P, Balla T, Sedat J W and Bourne H R (2000) Polarization of Chemoattractant Receptor Signaling During Neutrophil Chemotaxis. *Science* **287**: 1037-1040.

Siqueira-Junior JM, Peters R R, Brum-Fernandes A J and Ribeiro-do-Valle R M (2003) Effects of Valeryl Salicylate, a COX-1 Inhibitor, on Models of Acute Inflammation in Mice. *Pharmacological Research* **48**: 437-443.

Stephens L, Smrcka A, Cooke F T, Jackson T R, Sternweis P C and Hawkins P T (1994) A Novel, Phosphoinositide 3-Kinase Activity in Myeloid-Derived Cells Is Activated by G-Protein B γ -Subunits. *Cell* **77**: 83-93.

Stephens LR, Erdjument-Bromage H, Lui M, Cooke F, Coadwell J, Smrcka A V, Thelen M, Cadwallader K, Tempst P and Hawkins P T (1997) The G $\beta\gamma$ Sensitivity of a PI3K Is Dependent Upon a Tightly Associated Adaptor, P101. *Cell* **89**: 105-114.

Stoyanov B, Volinia S, Hanck T, Rubio I, Loubchenkov M, Malek D, Stoyanova S, Vanhaesebroeck B, Dhand R, Nurnberg B, Gierschik P, Seedorf K, Hsuan J J, Waterfield M D and Wetzker R (1995) Cloning and Characterization of G Protein-Activated Human Phosphoinositide-3 Kinase. *Science* **269**: 690-693.

Suire S, Condliffe A M, Ferguson G J, Ellson C D, Guillou H, Davidson K, Welch H, Coadwell J, Turner M, Chilvers E R, Hawkins P T and Stephens L (2006) G $\beta\gamma$ s and the

MOL #41780

Ras Binding Domain of P110 γ Are Both Important Regulators of PI3K γ Signalling in Neutrophils. *Nat Cell Biol* **8**: 1303-1309.

Welch HCE, Coadwell W J, Ellson C D, Ferguson G J, Andrews S R, Erdjument-Bromage H, Tempst P, Hawkins P T and Stephens L R (2002) P-Rex1, a PtdIns(3,4,5)P₃- and G[β][γ]-Regulated Guanine-Nucleotide Exchange Factor for Rac. *Cell* **108**: 809-821.

Wu D, Huang C K and Jiang H (2000) Roles of Phospholipid Signaling in Chemoattractant-Induced Responses. *J Cell Sci* **113**: 2935-2940.

Xanthou G, Duchesnes C E, Williams T J and Pease J E (2003) CCR3 Functional Responses Are Regulated by Both CXCR3 and Its Ligands CXCL9, CXCL10 and CXCL11. *Eur J Immunol* **33**: 2241-2250.

Yang YF, Mukai T, Gao P, Yamaguchi N, Ono S, Iwaki H, Obika S, Imanishi T, Tsujimura T, Hamaoka T and Fujiwara H (2002) A Non-Peptide CCR5 Antagonist Inhibits Collagen-Induced Arthritis by Modulating T Cell Migration Without Affecting Anti-Collagen T Cell Responses. *Eur J Immunol* **32**: 2124-2132.

Zhao T, Nalbant P, Hoshino M, Dong X, Wu D and Bokoch G M (2007) Signaling Requirements for Translocation of P-Rex1, a Key Rac2 Exchange Factor Involved in Chemoattractant-Stimulated Human Neutrophil Function. *J Leukoc Biol* **81**: 1127-1136.

MOL #41780

Footnotes:

- a) Unnumbered footnotes: Supported by NIH grants GM60286 (A.V.S.) and Postdoctoral Training grant in Cancer Biology (D.M.L.) the Johnson & Johnson Discovery Fund (A.V.S.) and an Arthritis Foundation Postdoctoral Fellowship (D.M.L.).
- b) A.V. Smrcka
University of Rochester, Department of Pharmacology and Physiology
601 Elmwood Ave., Box 711
Rochester, NY 14642
E-mail: alan_smrcka@urmc.rochester.edu
- c) Na

MOL #41780

Legends for figures:

Figure 1. Small molecule binding profiles. **(A)** Structures of M119, M119B, gallein, and fluorescein are shown. **(B)** M119 and gallein bind with comparable affinities in the competition phage ELISA. M119 and gallein were tested for their ability to inhibit binding of a phage displaying the peptide SIGK to the G $\beta\gamma$ “hot spot” as described previously (Bonacci *et al.*, 2006). Data shown is representative of 3 independent experiments, each in duplicate, +/- standard deviation. **(C)** Direct binding analysis of gallein bind to G $\beta\gamma$ by SPR. A representative experiment for gallein binding to bG $\beta_1\gamma_2$. Gallein binding was tested at sequentially higher nM concentrations indicated at the peak of each association followed by a dissociation phase with the compound removed between each addition. All data were fit with a kinetic titration model (Karlsson *et al.*, 2006) to give k_a and k_d values. In the experiment shown the fits resulted in $k_a=1130 \pm 17 \text{ M}^{-1}\text{s}^{-1}$ and $k_d=4.3 \pm .04 \times 10^{-4} \text{ s}^{-1}$. Pooled data from three separate experiments each are in Table 1.

Figure 2. “Hot spot” binding small molecules modulate key leukocyte functions. **(A)** M119 and gallein inhibit GFP-PH-Akt translocation. Differentiated HL60 cells stably expressing GFP-PH-Akt were challenged with 250 nM fMLP in the presence and absence of 10 μM of the indicated compounds. Translocation of GFP-PH-Akt to the plasma membrane was evaluated by western blot. Quantification shown below. ***P < 0.001 analysis of variance (ANOVA) is statistically different from control (PBS + vehicle). Western blot shown is representative of 3 independent experiments and quantitation contains data pooled from 3 independent experiments +/- SEM. **(B)** M119 and gallein

MOL #41780

block activation of Rac1. Differentiated HL60 cells were challenged with 1 μ M fMLP in the presence and absence of 10 μ M of the indicated compounds. Rac1 activation was assessed by western blots of affinity precipitated GTP-Rac1 from HL60 cell lysates. Western blot shown is representative of 3 independent experiments and quantitation contains data pooled from 3 independent experiments +/- SEM. *P<0.05 analysis of variance (ANOVA) is statistically different from control (DMSO only). n = 3. **(C, D)** M119 and gallein inhibit superoxide production in fMLP challenged HL60 cells. Differentiated HL60 cells were challenged with 250 nM fMLP or 250 nM PMA in the presence and absence of 10 μ M compounds or 100 nM Wortmannin (Wtmn). NADPH oxidase activity was determined after reaction with NBT by absorbance at 540 nM. Data shown is contains data pooled from 3 independent experiments (each in duplicate) +/- SEM. *P<0.05 analysis of variance (ANOVA) is statistically different from control (DMSO only).

Figure 3. “Hot spot” binding small molecules inhibit GPCR-coupled chemoattract-dependent chemotaxis. **(A)** M119 and gallein inhibit fMLP-induced chemotaxis in differentiated HL60 cells. Differentiated HL60 cells (200k) were pretreated with 10 μ M of the indicated compound, challenged with 250 nM fMLP and assayed for chemotaxis in a Boyden chamber for 1 h at 37 °C. Chemotaxis was quantified by counting Diffquik® stained cells in 3 random microscope fields, subtracting out background cells (0-10 cells) in the absence of chemoattractant to obtain total transmigrated cells (~125 cells fMLP + vehicle) and represented as the percent of fMLP treated control cells. ***P < 0.001

MOL #41780

ANOVA is statistically different from control. Data shown pooled from 3 independent experiments, each in duplicate, +/- SEM. **(B)** Neither M119 nor gallein block GM-CSF (1 μ M) induced chemotaxis in a Boyden chamber. Chemotaxis was quantified as above by subtracting out background cells (0-10 cells) in the absence of chemoattractant to obtain total transmigrated cells (~100 cells GM-CSF + vehicle) and represented as the percent of GM-CSF treated control cells. No statistically significant difference from control was seen by ANOVA. Data shown are pooled from 2 independent, each in duplicate, +/- SEM. **(C)** M119 and gallein inhibit fMLP- and IL-8-induced chemotaxis in human neutrophils in a Boyden chamber. Primary human neutrophils were isolated from whole blood to \geq 80% purity. Neutrophils (200k) were pre-treated with gallein (10 μ M), M119 (10 μ M), M119B (10 μ M), or wortmannin (wtmn.) (1 μ M) and then challenged with 250 nM fMLP or 10 nM IL-8 to evaluate chemotaxis in a Boyden chamber for 1 h at 37 $^{\circ}$ C. Chemotaxis was quantified as above by subtracting out background cells (0-10 cells) to obtain total transmigrated cells (fMLP ~100 cells and IL-8 ~175 cells) and represented as the percent of chemoattractant treated control cells. ***P < 0.001 ANOVA is statistically different from control. NS; not statistically different from control. Data are mean +/- SEM. Data shown is pooled from 3 independent experiments, each in duplicate, +/- SEM. **(D)** Gallein dose-dependently inhibits human neutrophil chemotaxis in a Boyden chamber. Primary human neutrophils were isolated and treated (250 nM fMLP +/- gallein) as described above. Chemotaxis was quantified as above by subtracting out background cells to obtain total transmigrated cells and represented as the percent of fMLP treated control cells. Data shown are pooled from 2 independent experiments, each in duplicate, +/- SEM.

MOL #41780

Figure 4. G $\beta\gamma$ “hot spot” binding small molecules inhibit neutrophil recruitment and acute phase inflammation *in vivo*. **(A)** Gallein inhibition of carrageenan-induced paw edema. Male 35-40 gram mice were injected IP with 100 mg/kg gallein or 2.5 mg/kg indomethacin in PBS 1 h prior to subplantar injection of 50 μ l of 2% carrageenan (Cg) into the test paw. The contralateral paw was injected with saline as control. Each paw was measured 3 times every 2 hours. Δ Paw thickness was quantified by subtracting the average thickness of the contralateral paw from the average thickness of the test paw. Each point represents the average paw thickness of 4 mice, each measurement done in duplicate. Data shown is representative of >3 independent experiments. Data are mean \pm SEM. **(B)** Gallein inhibits carrageenan-induced paw edema in a dose-dependent manner. Mice (4 mice per plotted point) were treated and quantified as described above. Data are mean \pm SEM. **(C)** Neutrophil recruitment is attenuated by gallein. Mice (4 mice per plotted point) were treated as described above. Two hours post carrageenan injection paws were severed and the number of neutrophils contained within edematous fluid was determined. Data are mean \pm SEM. ***P < 0.001 and **P < 0.01 ANOVA are statistically different from control. **(D)** Paw swelling is reduced by gallein. Mice (4 mice per plotted point) were treated as described above. Two hours post carrageenan injection paws were severed and the volume of edematous fluid was determined. ***P < 0.001 ANOVA is statistically different from control.

MOL #41780

Figure 5. *Gallein is effective with oral administration.* Male (35-40 gram) mice were dosed by oral gavage with 30 mg/kg gallein 1 h prior to challenge with 2% carrageenan. Methods are as described in Figure 4. Each bar represents the average paw thickness of 4 mice at 3 h post carrageenan injection, each measurement done in duplicate. Data are mean \pm SEM. ***P < 0.001 and **P < 0.01 ANOVA are statistically different from vehicle. NS; not statistically different from control. Data shown is representative of 2 independent experiments.

MOL #41780

Table 1. Equilibrium and kinetic binding constants for small molecule binding to $\beta_1\gamma_2$ calculated from surface plasmon resonance analysis and ELISA competition.

	K_d nM ^a	K_{on} ($\times 10^3 M^{-1} S^{-1}$)	K_{off} ($\times 10^{-4} S^{-1}$)	ELISA IC ₅₀ nM
Gallein	422±49	0.99±0.11	4.09±.09	241±24
Fluorescein	NB			

^aValues are mean +/- SE from 3 separate experiments. NB = no binding detected.

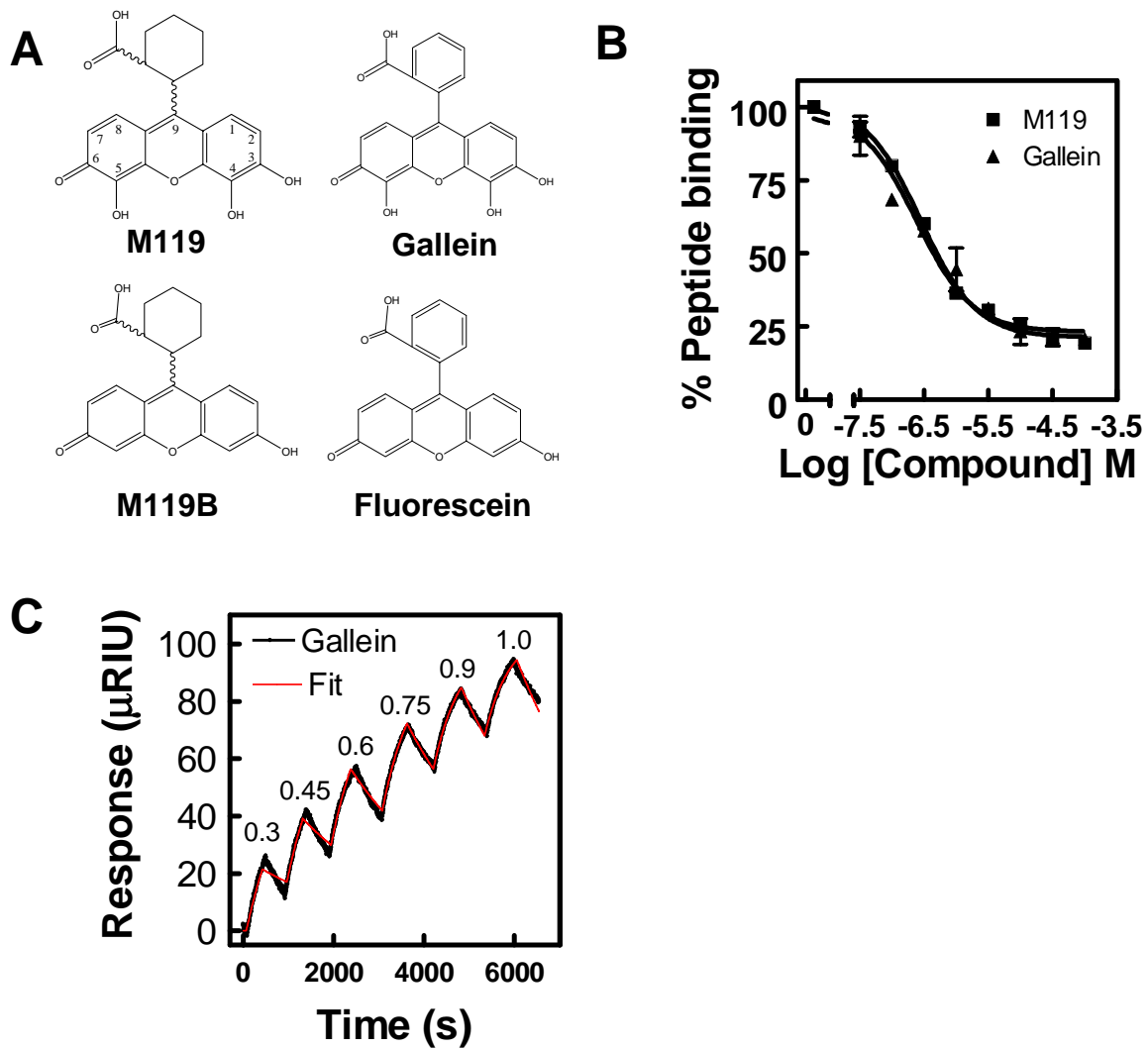


Figure 1.

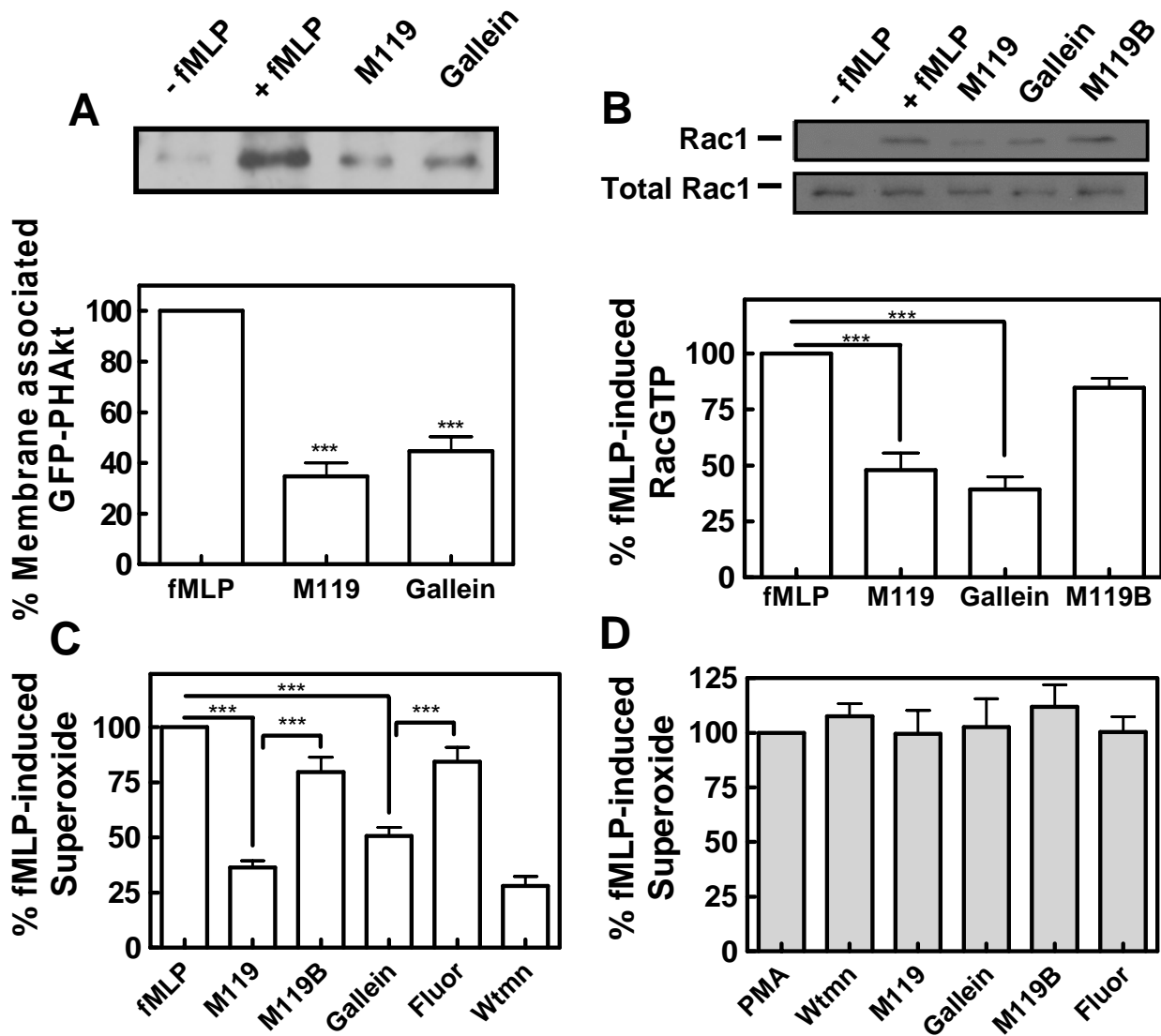


Figure 2.

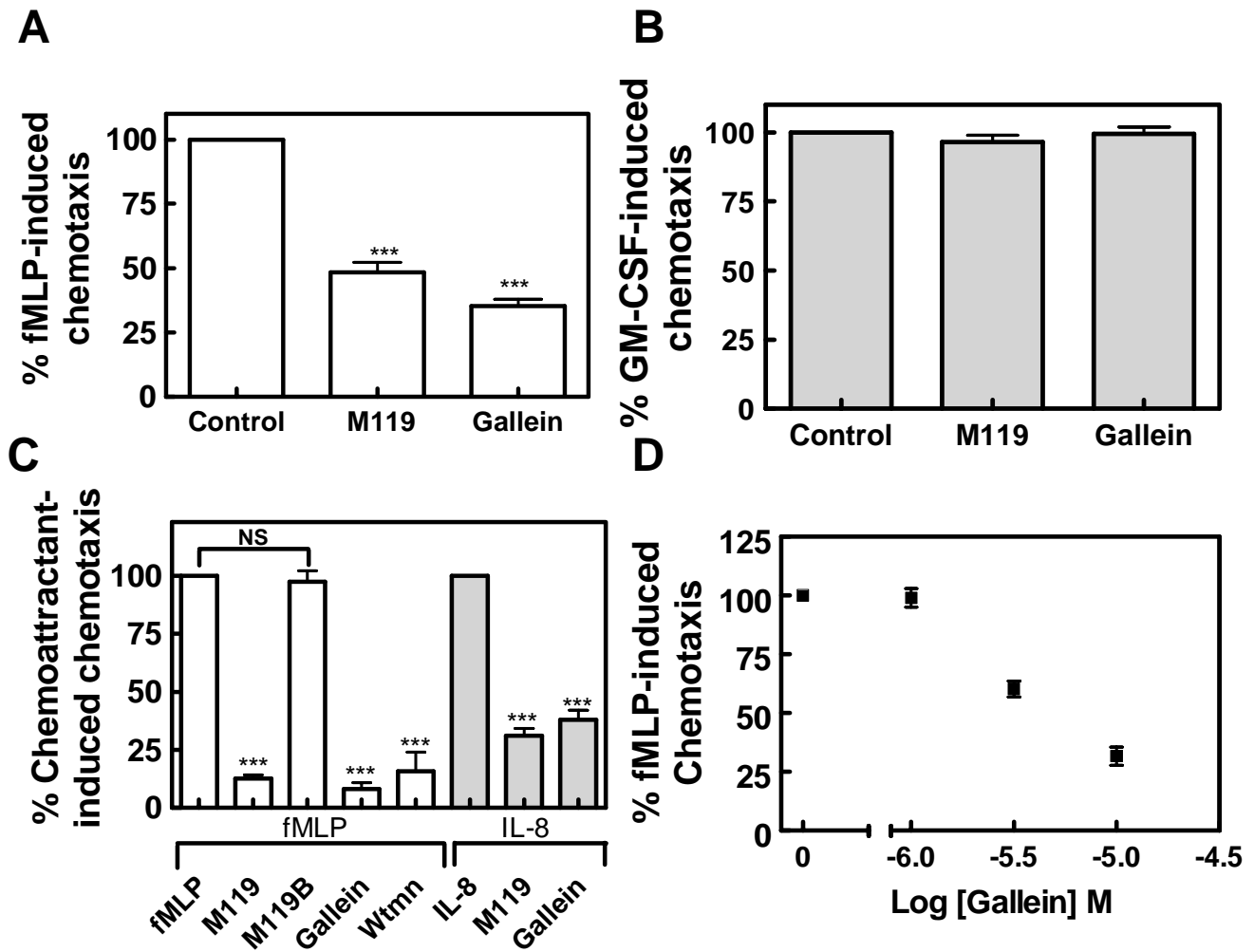


Figure 3.

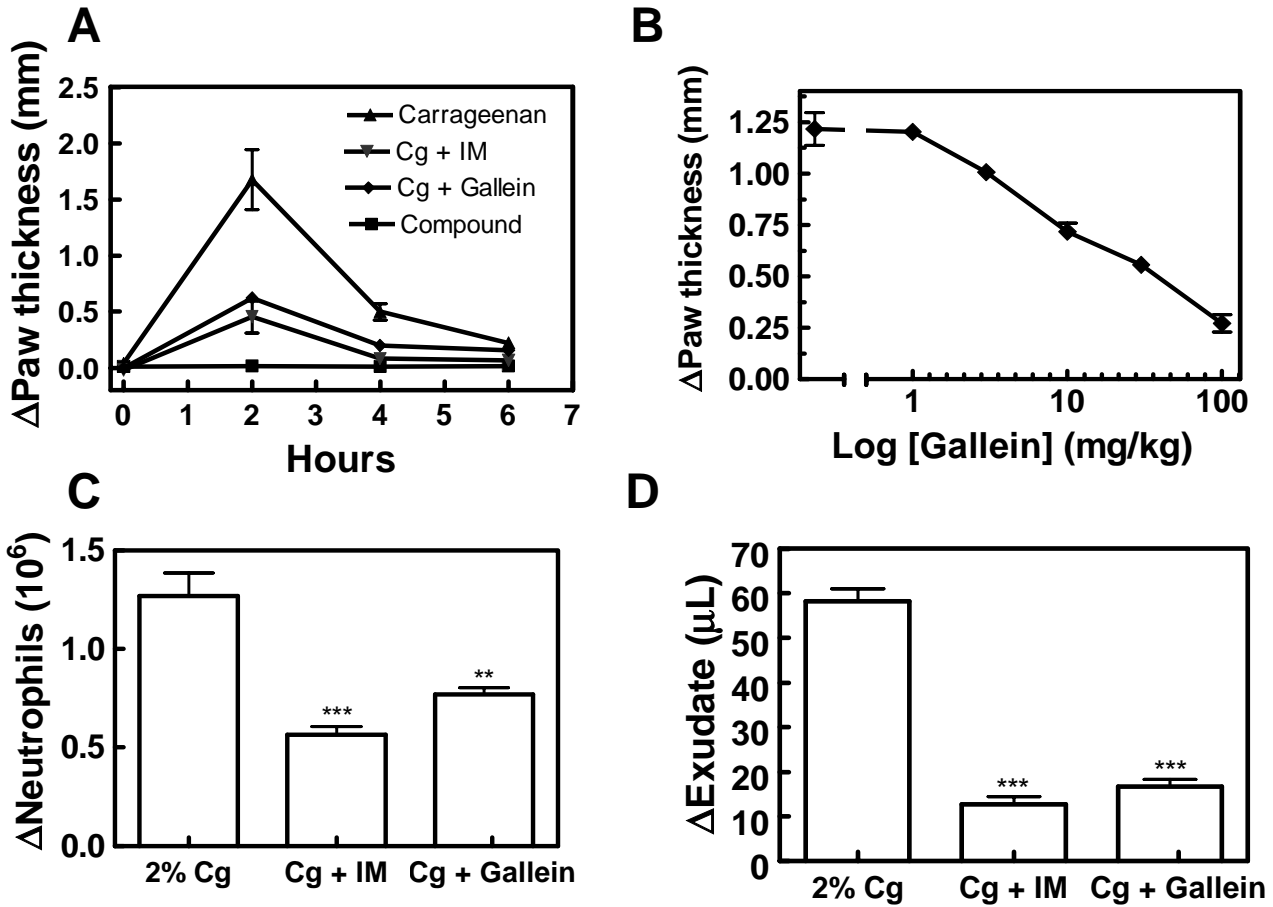


Figure 4.

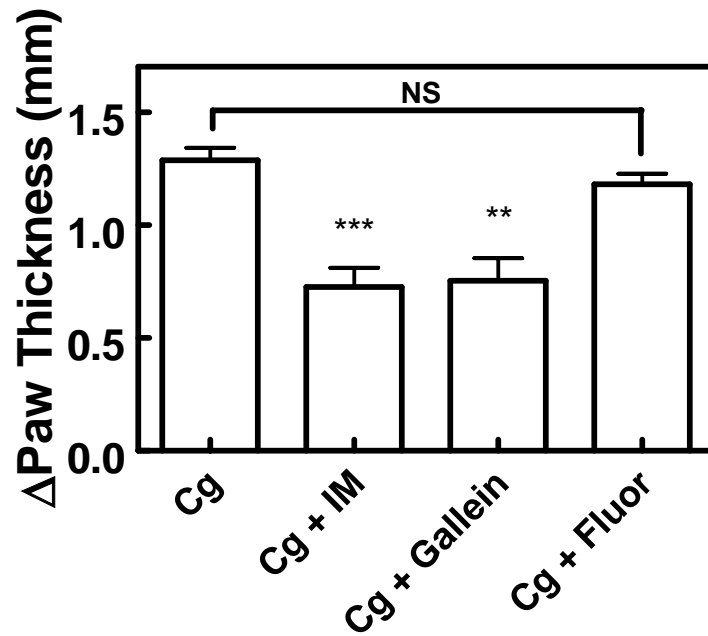


Figure 5.